International Journal of Innovative Research and Scientific Studies, 8(7) 2025, pages: 25-35

IJIRSS
International Journal of Innovative Research & Scientific Studies

ISSN: 2617-6548

URL: www.ijirss.com

Effect of small gap between tube and suction box on crevice corrosion formation of the dewatering tube

Adimas Aprilio Hardinanto[1], Amin Suhadi[2*], Anne Zulfia[1], Eka Febriyanti[2], Muhammad Syahril[2]

[1]*Metallurgy and Materials Department, Faculty of Technology, University of Indonesia, jl. Lingkar Pondok Cina, Depok – Jabar 16424, Indonesia.*
[2]*Research Center for Structural Strength Technology, National Research and Innovation Agency, Gedung 220 KST BJ.Habibie, Tangsel, 15314, Indonesia.*

Corresponding author: Amin Suhadi (*Email: amin001@brin.go.id*)

Abstract

Dewatering tube is a crucial equipment used to separate water and solids during papermaking process. The tube made of SS 316L stainless steel, responsible for supplying fresh water, failed during operation. The purpose of this research was to determine the cause of failure to prevent similar issues in the future. Methods used in this research mainly implements root cause analysis while considering all possible aspects contributing to the failure. Pitting Resistance Equivalent Number of 23.499 was obtained, indicating acceptable value of SS 316L localized corrosion resistance. However, the results of the examination indicated that the failure of the dewatering tube was caused by crevice corrosion. The crevice corrosion was formed due to trapped chlorine-containing water in the gap between the tube and suction box. The chlorine content of 3.36 wt% was confirmed by EDS. The presence of chlorine deposits in the gap between suction box, in combination with operating temperature (70 – 80°C) and environment (pH 3.5 to 4.5) caused the localized corrosion reaction to occur, ultimately leading to tube leakage. The study's results provide valuable insights for industries to mitigate the risk of similar issues of equipment that operates in corrosive environment in conjuction with elevated temperature.

Keywords: Corrosion, Crevice, Dewatering, Failure, Tube.

DOI: 10.53894/ijirss.v8i7.10398
Funding: This study received no specific financial support.
History: Received: 13 August 2025 / **Revised:** 15 September 2025 / **Accepted:** 18 September 2025 / **Published:** 1 October 2025

Competing Interests: The authors declare that they have no competing interests.
Authors' Contributions: All authors contributed equally to the conception and design of the study. All authors have read and agreed to the published version of the manuscript.
Transparency: The authors confirm that the manuscript is an honest, accurate, and transparent account of the study; that no vital features of the study have been omitted; and that any discrepancies from the study as planned have been explained. This study followed all ethical practices during writing.
Acknowledgments: The authors wish to acknowledge the management of the Laboratory of Strength of Structure (KS-BRIN) and all laboratory staff for their support and provision of facilities. We also extend our gratitude to Department of Metallurgical and Materials Engineering University of Indonesia for their guidance throughout this work.
Publisher: Innovative Research Publishing

1. Introduction

Pulp and paper mills are highly complex facilities that integrate various process areas to convert wood into the final product. The processing options and type of wood used are often determined by the desired final product. Pulping and papermaking rely on capital-intensive technical equipment and high-tech, high-speed paper machines that can produce rolls of paper at speeds of up to 2,000 meters per minute, with a web width exceeding 8 meters [1]. Dewatering is a process used to separate water and solids during stock preparation and the papermaking stage. If any component of this unit fails, the system will not function properly [2-4]. In this research, the tube responsible for streaming fresh water during the dewatering process failed during operation. The tube was clamped to the suction box and, although it was not immersed during the process, it was exposed to splash water from the surrounding area with a pH of 3.5 to 4.5. The tube corroded after only three months of operation. The failed tube was then brought to the laboratory for analysis to determine the root cause of the failure.

2. Material and Methods

The material of the tube investigated is AISI 316L stainless steel, with a diameter of 15.875 mm and a thickness of 1.71 mm. This tube was taken from a part of the dewatering system on a papermaking machine, as shown in Figure 1.

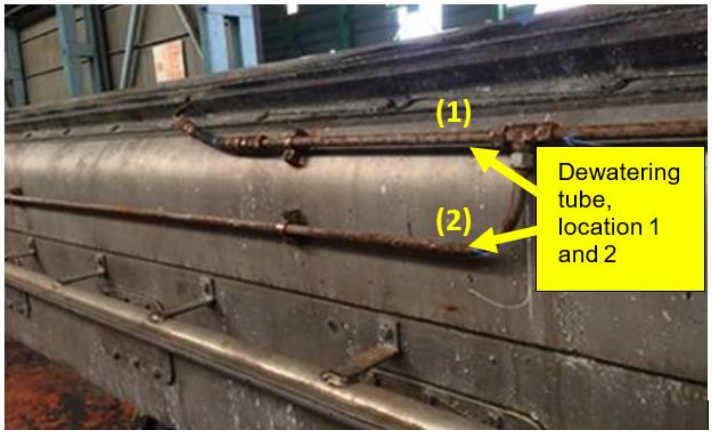

Figure 1.
Location of the tube examined in the laboratory to determine the root cause of the failure. Tubes on location 1 and 2 are attached on the same suction box.

The operational conditions of the dewatering system from which the tube was taken are listed in Table 1.

Table 1.
Technical Operational Data.

Parameters	Remark
Material	AISI 316 L
Operational pressure	1 atm
Operational temperature	70 – 80 °C
Environment	Wet environment

The examination method employed in this research involves implementing root cause analysis, which includes macro-fractography, metallography, chemical analysis, hardness testing, scanning electron microscopy, and energy-dispersive X-ray spectroscopy [5, 6]. The objective of these tests and examinations is to gather valuable information regarding the initial cause of the failure. The procedure and objective of each test are as follows:

- Visual examination was conducted to identify damage characteristics and determine the preparation steps for further analysis. This method involved a detailed assessment of the sample's condition, including the location of damage, which was documented using a digital camera. The failed tube was visually inspected and photographed in its as-received condition.
- Macrographic examination was performed to identify the initial crack, determine the direction of crack propagation, assess the fracture mode, and detect any material defects around the fracture area. This test utilized an optical stereo microscope, and specimens were carefully prepared from the fracture surface, with particular attention given to areas suspected of containing the initial crack.
- Micrographic (metallographic) examination was carried out to explore finer details of the fracture area, focusing on microstructure and its evolution, as well as micro defects, micro cracks, and other micro discontinuities that may have contributed to the fracture. Optical microscopes were used to analyze cross-sections and longitudinal planes of the tube, allowing for the monitoring of microstructural changes.
- SEM and EDAX analysis were performed to examine the cracks' surface in greater detail and to determine the elemental composition of the fracture surface. This examination aims to identify elements that might exhibit aggressive characteristics and contribute to the damage or initial failure.

- The chemical composition analysis involves examining the elemental content of the base material of the tube using a spark spectrometer. The results are then compared with the specified composition outlined in the reference standards.
- The hardness test was performed to verify whether the material meets the specified classification. The test was conducted using a Vickers hardness tester.
- Tensile tests were conducted using universal testing machines to assess the material's current strength properties.

All results from these examinations and tests were rigorously analyzed to identify the primary factor responsible for the initial crack or leak, as well as any contributing factors that accelerated further degradation of the tube [7, 8]. This approach includes examining all potential factors that may have contributed to the tube's failure [5]. Typically, major sources of failure can stem from issues such as incorrect design, manufacturing defects, improper installation, incorrect operational parameters, and unsuitable material specifications [9, 10]. In this research, design, manufacturing, and installation aspects were not examined, as the unit's reliability had been confirmed by the owner prior to installation, affirming the integrity of these factors. Therefore, the research focused exclusively on operational factors. Once the most dominant factor was identified, further examinations were conducted to uncover additional valuable scientific insights.

3. Results and Discussion

3.1. Result

The results from all tests and examinations provide valuable information that can guide the investigation into the primary cause of the tube failure.

3.1.1. Visual and Macrographic Examination

The visual examination clearly shows that the investigated tube is heavily corroded by general corrosion on its outer surface, as depicted in Figure 2.

Figure 2.
Visual examination of the failed tube (Location 1) reveals that the majority of the outer surface is covered by corrosion products.

Higher magnification of specific areas facing the suction box either at location-1 or location-2 reveals evidence that the corrosion process has penetrated the tube's thickness, forming longitudinal notches. These notches are present at multiple observation locations, as shown in Figure 3.

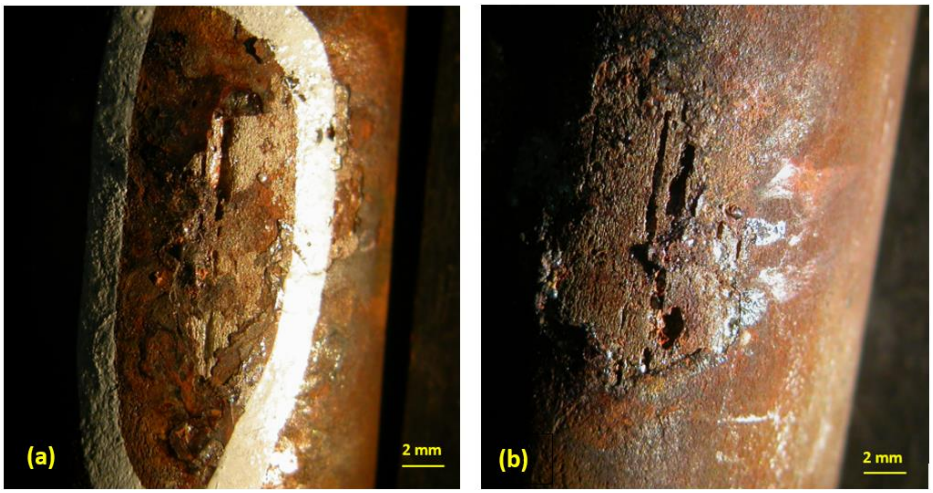

Figure 3.
Observation of notches on the tube surfaces at different locations facing the suction box: (a) Location 1 and (b) Location 2.

However, no corrosion products or crevices are found on the inner tube surface, which remains clean and in good condition (Figure 4).

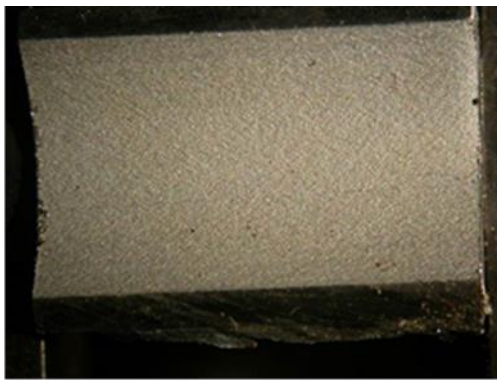

Figure 4.
Visual examination of the inner tube surface shows no corrosion products and it remains in good condition.

Macrographic examination of the cross-section at location-1 confirmed that the notches originated from the outer surface of the tube, as depicted in Figure 5a.

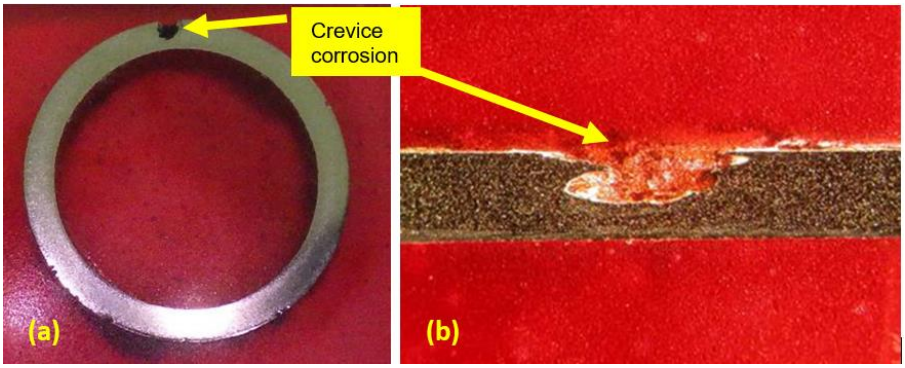

Figure 5.
Cross-sectional examination of the tube at Location 1 (a) and longitudinal section at Location 2 (b) reveal the formation of notches originating from the outer surface.

A similar phenomenon occurred on the longitudinal section of location-2, which was also facing the suction box (Figure 5b). These observations confirm that the main cause of failure originated from the outer surface of the tube, while the inner surface remains free from corrosion and in good condition. There is no evidence of thinning or leakage caused by other mechanisms such as mechanical impact, overloading, erosion, bulging, or thermal deformation. Therefore, the primary cause of failure appears to be the formation of a crevice on the outer surface [11, 12].

3.1.2. Microstructure Examination

The metallographic examination of the bulk area revealed that the microstructure of the tube is austenitic, which is typical of 316L stainless steel (Figure 6) [11]. Therefore, the failure of this tube cannot be attributed to incorrect material selection. Further examination of the microstructure at the leakage area confirms that the notch was formed on the outer surface of the tube.

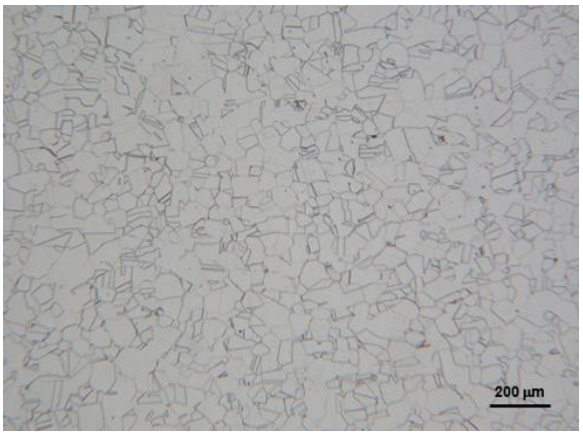

Figure 6.
Microstructure of the bulk tube material is austenitic, it is in accordance with 316 L stainless steel microstructure.

There is no evidence indicating that the formation of the notch was caused by mechanisms such as erosion or mechanical impact, other than crevice corrosion. This is supported by the presence of black deposits on the notch surface and the observation of truncated grain structure along the notch surface (Figure 7).

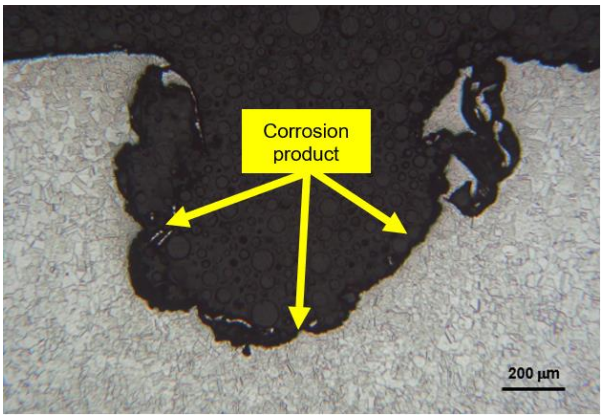

Figure 7.
Higher magnification using metallography technic revealed that the notch area is covered by corrosion products.

Moreover, the wide and deep dimensions of the notch contour are typical of crevice corrosion attack [7, 12, 13]. Microstructure examination revealed no indications of other contributing factors to the leakage, such as microcracks, inclusions, or micro defects.

3.1.3. Chemical and Hardness Testing Result

Chemical and hardness tests were conducted on the bulk material to verify conformity to the AISI SS 316L standard as specified by the factory. The results indicated that the tube material composition is in accordance with the specifications (Table 2).

Table 2.
Chemical Composition Test Result of Tube Material.

Element	Result Wt %	Specification Wt%
Cr	16.8	16.00-18.00
Ni	10.8	10.00-14.00
Mo	2.03	2.00-3.00
C	0.016	0.03 max
Mn	1.19	2.00 max
P	0.06	0.045 max
S	0.01	0.03 max
Si	0.41	0.75 max
N	NA	0.1 max
Fe	Balance	Balance

This finding is corroborated by the hardness test, which yielded a maximum value of 155 HV (Table 3).

Table 3.
Vickers Hardness Test Result on the Cross-Section of the Tube.

Point No.	HV	Specification
1	130	155 HV Max.
2	139	
3	134	
4	138	
5	137	
Average	135.6	

3.1.4.SEM and EDX Testing Result

Crevice evidence was also observed using Scanning Electron Microscopy (SEM), which revealed a wide and deep notch characteristic of crevice failure and the crevice wall is covered by corrosion product (Figure 8 a and b). Energy Dispersive X-Ray (EDX) analysis of the black deposits on the notch surface indicated high oxygen content and identified the presence of corrosive chlorine (Cl) on the surface. It is confirmed that the deposit on the notch surface is a corrosion product (Figure 9 and Table 4).

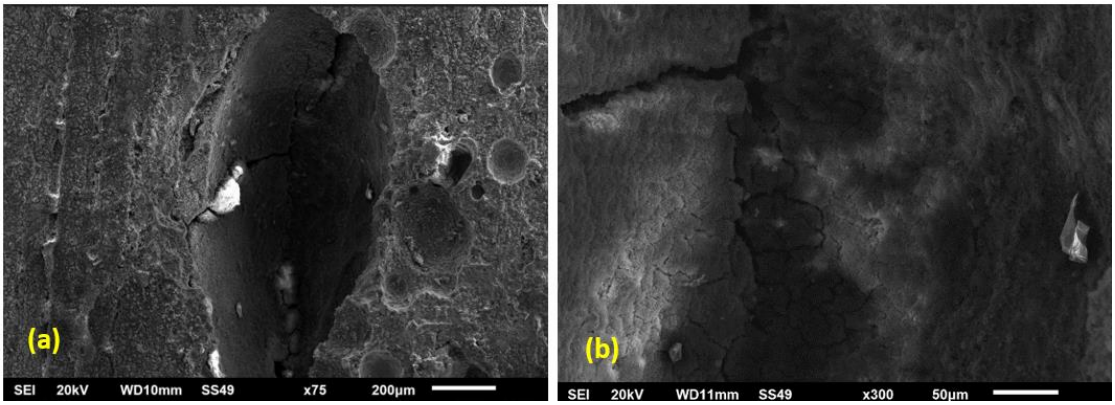

Figure 8.
Scanning Electron Microscopy (SEM) examination of the notch area shows that the notch is characteristic of crevice corrosion (a) and the crevice wall is covered by corrosion product (b).

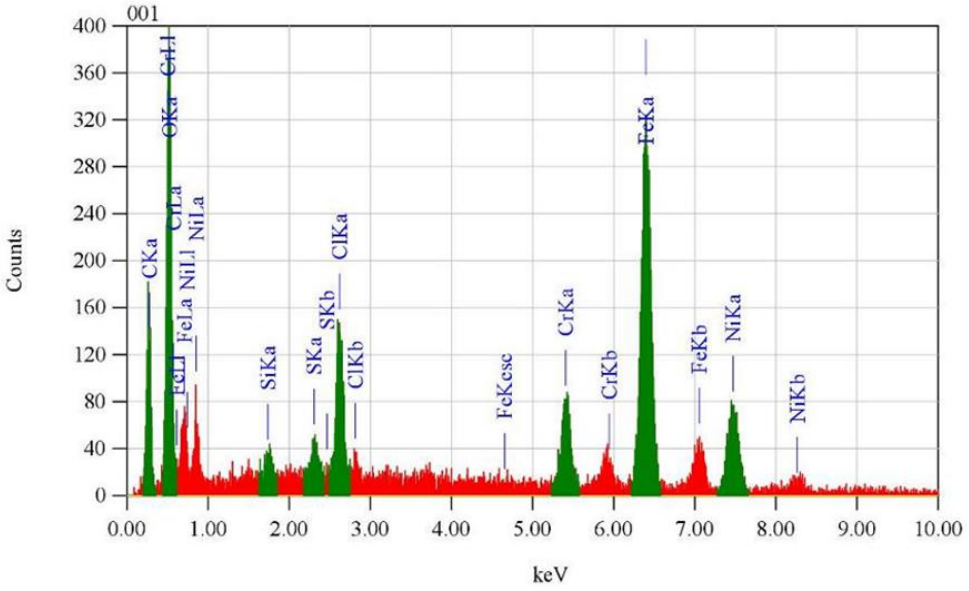

Figure 9 Energy Dispersive X-Ray (EDX) analysis of the notch surface indicates high oxygen content, representing corrosion products, and reveals the presence of the corrosive element chlorine (Cl).

Table 4.
EDX analysis results at the notch surface.

Element	Mass %
C	22.46
O	29.19
Si	0.50
S	0.64
Cl	3.36
Cr	4.72
Fe	29.04
Ni	10.10

3.2. Discussion

3.2.1.Failure Initiation Analysis

Stainless steel SS 316L is a common material used in the paper manufacturing industry due to its high resistance to general corrosion in corrosive environments and its strength to support high loads. However, passive alloys, particularly those in the stainless steels group, are more susceptible to crevice corrosion under specific conditions compared to materials that exhibit more active behaviour [14, 15]. Crevice corrosion is a type of localized corrosion that occurs within confined spaces or crevices formed between two surfaces. It can affect various alloys, including stainless steel, aluminium, titanium, and copper. The resistance to crevice corrosion can vary among alloys depending on environmental parameters such as temperature, chloride concentration, pH, and oxygen content [3, 16]. The metallographic examination of the tube's cross-section reveals that the damage is characteristic of crevice corrosion failure (Figures 5 and 7). Considering all the evidence obtained, it is obvious that the notch is a result of crevice corrosion [11, 17].

In this research, the failed tube was clamped to the suction box with an approximate 2 mm gap in between (Figure 1). The presence of such narrow gaps between the suction box and the tube can lead to localized corrosion at this site (Figure 10) [11].

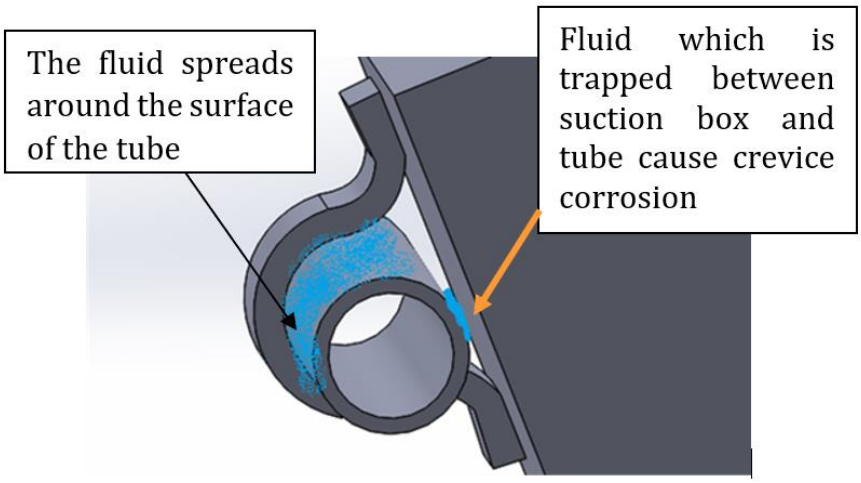

Figure 10.
Fluid trapped between the tube and the suction box promote localized corrosion reaction.

Crevice corrosion can occur when water splashed from the dewatering process, along with dirt, becomes trapped in these narrow gaps, leading to the breakdown of the passive surface layer within the crevices or shielded areas. The common mechanism behind all types of crevice corrosion is the development of a localized environment that can differ significantly from the bulk environment, often resulting from the establishment of oxygen differential cells. Oxygen ingress in the process and production system can be detrimental to corrosion-resistant alloys. This occurs when oxygen within the crevice electrolyte is consumed, while the surrounding exposed surface has ready access to oxygen and becomes cathodic relative to the crevice area (Figure 11) [18, 19].

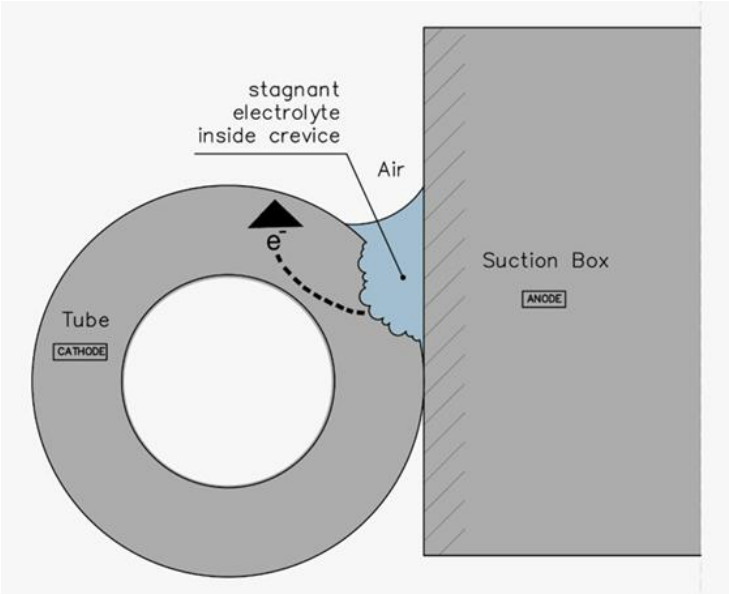

Figure 11.
The role of oxygen in the initiation of crevice corrosion on the tube.

3.2.2. Effect of Atmospheric Hydrogen Potential (pH)

It is well known that a low pH level can reduce the stability of the passive layer on stainless steel, which serves as the corrosion-resistant component. This passive layer is composed of chromium oxide, formed by the oxidation of chromium in the atmosphere. It has a regenerative characteristic, allowing it to automatically recover when scratched. As a result of the reduced stability of this passive layer, stainless steel becomes prone to crevice corrosion, particularly in areas where the electrolyte solution is trapped. When the passive layer is damaged, it is difficult to regenerate a new layer because it cannot come into contact with atmospheric oxygen due to obstruction by the solution. This condition is exacerbated by the fact that the pH decreases further due to the dissolution of chromium in the electrolyte at the crevice location when the passive layer is damaged [20]. Given that the operational pH is between 3.5 and 4.5, it can be confirmed that the passive layer of

SS 316L is in an unstable condition. The Pourbaix diagram for chromium (Figure 12) indicates that, under these conditions, it is difficult to regenerate the passive layer. As a result, crevice corrosion may continue to progress [11].

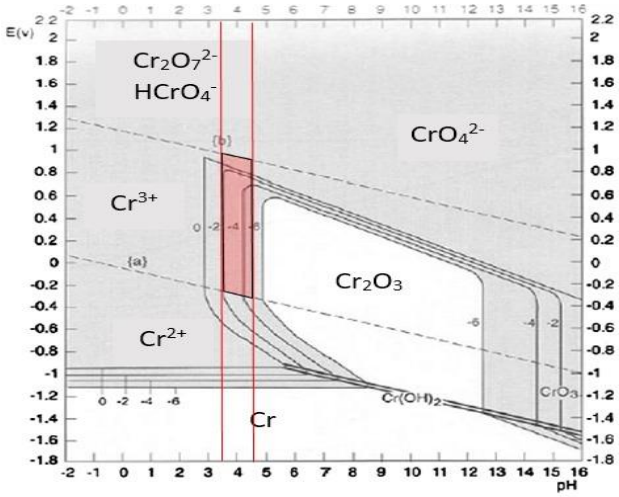

Figure 12.
The Chromium Pourbaix diagram shows that the passive layer (Cr_2O_3) becomes ionized to Cr^{3+} under pH 3.5 conditions Kain [11].

3.2.3. Effect of Atmospheric Hydrogen Potential (pH)

Temperature is a crucial factor in corrosion reactions, with the corrosion rate typically doubling for every 10°C increase in temperature. For specific stainless steels, localized corrosion can initiate only above a critical temperature; however, this critical temperature can be lower in environments with high chlorine concentration [21, 22]. As shown in Figure 13, SS316L material with approximately 2.8 weight % molybdenum (Mo) has a critical temperature of only 13°C in a chlorine-containing environment [13, 23].

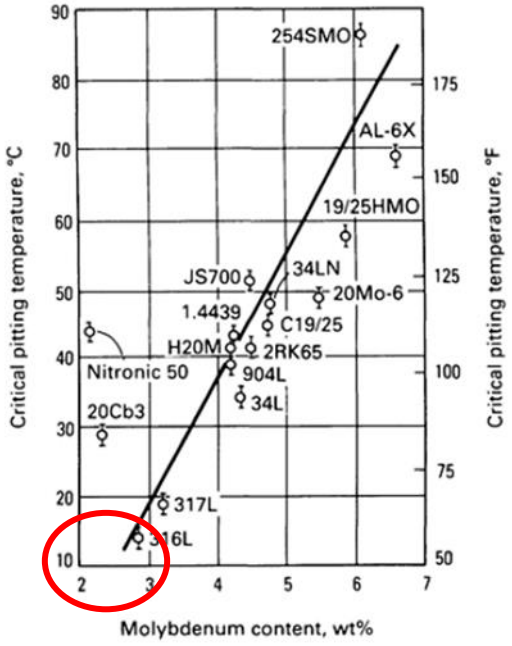

Figure 13.
The effect of molybdenum (Mo) on various stainless steels types in an Fe Cl_3 environment with critical pitting or crevice Kain [11].

It can be confirmed that the tube investigated, with a 2.03% Mo content and operated at temperatures around 70–80°C, is prone to localized corrosion attacks. Additionally, another approach to assess corrosion resistance is through the Pitting Resistance Equivalent Number (PREN), which depends on the chemical alloy content of the material. The PREN can be calculated using the following equation [11]:

$$PREN = \%Cr + 3.3\ (\%Mo) + X(\%N) \quad (1)$$

where x is typically given as either 16 or 30

Although this relationship was developed to rank pitting resistance, it also provides a relative ranking of a stainless steel's crevice corrosion resistance. The calculation from the chemical composition test of the tube indicates a PREN of

approximately 23.499 which indicates the acceptable value of SS316L pitting resistance. When this data is compared to the critical pitting temperature (CPT) and critical crevice corrosion temperature (CCT), as shown in Figure 14, it is evident that SS316L has low CCT (-10°C). It confirms that crevice corrosion is likely to occur when operating temperature is above CCT. It is important to remember that crevice corrosion can occur at lower temperatures than pitting corrosion because less effort is required to initiate a pit within the geometric crevice [24].

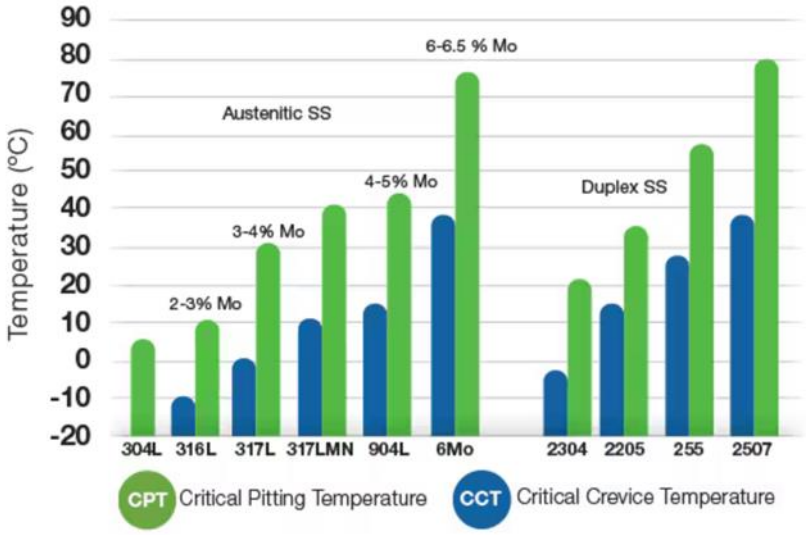

Figure 14.
Critical pitting temperature (CPT) and critical crevice corrosion temperature (CCT) for various austenitic and duplex stainless steels, measured according to ASTM G48 in 10% ferric chloride Wei, et al. [4].

3.2.4. Effect of of Chlorine Content

The presence of chloride ions significantly promotes crevice corrosion. Higher chlorine content in the area creates a chemically aggressive environment where corrosion-causing ions cannot readily diffuse out of the crevice. In such conditions, the entire surface within the crevice can corrode at an accelerated rate [25]. As shown in Figure 15, crevice corrosion of 316L stainless steel begins to occur in water with chloride content as low as 2000 ppm.

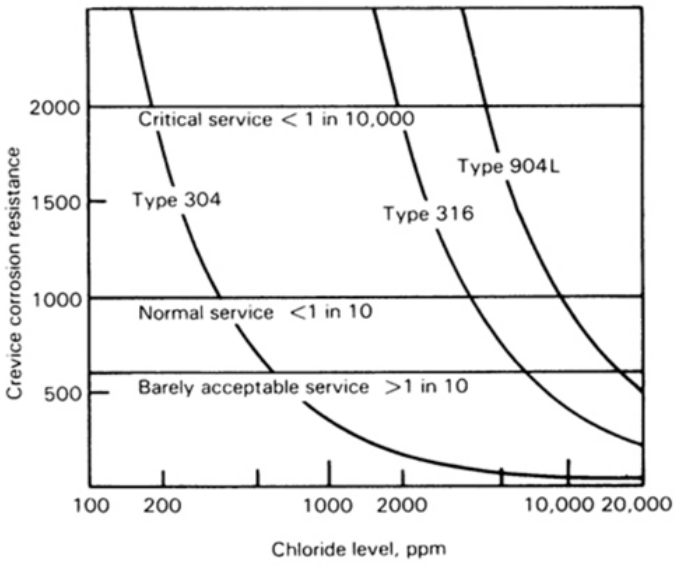

Figure 15.
Probability of crevice corrosion occurring in water containing chlorine Yang, et al. [26].

It is important to consider that the watering system in the pulp industry contains chlorine concentrations and operates at temperatures above the critical passive layer strength of stainless steel. Therefore, crevice corrosion is readily initiated [26-28].

4. Conclusions

Based on the results of all tests and examinations, it can be concluded that the failure of the dewatering tube was caused by crevice corrosion. This corrosion was initiated by water splashed from the dewatering process, combined with

dirt, and trapped in the narrow gaps between the suction box and the tube. The crevice corrosion was further accelerated by the presence of chlorine and the low pH of the environment.

References

[1] E. S. Abd El-Sayed, M. El-Sakhawy, and M. A.-M. El-Sakhawy, "Non-wood fibers as raw material for pulp and paper industry," *Nordic Pulp & Paper Research Journal*, vol. 35, no. 2, pp. 215-230, 2020. https://doi.org/10.1515/npprj-2019-0064

[2] T. Meyer, P. Amin, D. G. Allen, and H. Tran, "Dewatering of pulp and paper mill biosludge and primary sludge," *Journal of Environmental Chemical Engineering*, vol. 6, no. 5, pp. 6317-6321, 2018. https://doi.org/10.1016/j.jece.2018.09.037

[3] J. E. Naicker, R. Govinden, P. Lekha, and B. Sithole, "Transformation of pulp and paper mill sludge (PPMS) into a glucose-rich hydrolysate using green chemistry: Assessing pretreatment methods for enhanced hydrolysis," *Journal of Environmental Management*, vol. 270, p. 110914, 2020. https://doi.org/10.1016/j.jenvman.2020.110914

[4] W. Wei, Z. Tian, Q. Wang, J. Chen, G. Zhang, and L. Lucia, "Understanding the effect of severity factor of prehydrolysis on dissolving pulp production using prehydrolysis kraft pulping and elemental chlorine-free bleaching sequence," *BioResources*, vol. 15, no. 2, p. 4323, 2020.

[5] A. Suhadi, E. Febriyanti, and L. Sari, "The role of failure analysis on maintaining reliability of oil refinery for sustainable development goals," presented at the IOP Conference Series: Materials Science and Engineering, 2021.

[6] A. Suhadi, A. Aprilio, and E. Febriyanti, "Structural strength degradation of oil and gas refinery equipment: Case study: Heat exchanger tubes of hydrocarbon vapor," *Evergreen*, vol. 10, no. 4, p. 2449-2455, 2023. https://doi.org/10.5109/7162005

[7] J. W. Oldfield, "Test techniques for pitting and crevice corrosion resistance of stainless steels and nickel-base alloys in chloride-containing environments," *International Materials Reviews*, vol. 32, no. 1, pp. 153-172, 1987. https://doi.org/10.1520/G0048-11R20E01

[8] M. Syahril, A. Suhadi, E. Febriyanti, Y. Afandi, and F. Karuana, "Evaluation of refinery unit tube heater condition after±15 years in service by NDT methods," presented at the AIP Conference Proceedings, 2024.

[9] A. ElJersifi *et al.*, "Failure analysis of a stainless steel component operating inside an acid leaching reactor," *Engineering Failure Analysis*, vol. 149, p. 107256, 2023. https://doi.org/10.1016/j.engfailanal.2023.107256

[10] J.-h. Zhai, B.-b. Sun, and Y. Zhou, "Failure analysis on 304 stainless steel tube of semi water gas preheater in coal chemical plant," *Engineering Failure Analysis*, vol. 125, p. 105443, 2021. https://doi.org/10.1016/j.engfailanal.2021.105443

[11] R. Kain, "ASM metals handbook ASM metals handbook volume13-corrosion," *ASM International*, vol. 13, no. 11, pp. 685--705, 1992.

[12] E. M. Costa *et al.*, "Crevice corrosion on stainless steels in oil and gas industry: A review of techniques for evaluation, critical environmental factors and dissolved oxygen," *Engineering Failure Analysis*, vol. 144, p. 106955, 2023. https://doi.org/10.1016/j.engfailanal.2022.106955

[13] L. Li, J. Yan, J. Xiao, L. Sun, H. Fan, and J. Wang, "A comparative study of corrosion behavior of S-phase with AISI 304 austenitic stainless steel in H2S/CO2/Cl-media," *Corrosion Science*, vol. 187, p. 109472, 2021. https://doi.org/10.1016/j.corsci.2021.109472

[14] A. Lanzutti, F. Andreatta, M. Magnan, A. Gerolin, and L. Fedrizzi, "Unexpected failure of cast superduplex stainless steel exposed to high chlorides containing water: From failure analysis to corrosion mechanisms settlement," *Engineering Failure Analysis*, vol. 136, p. 106196, 2022. https://doi.org/10.1016/j.engfailanal.2022.106196

[15] M. Hazra and K. Balan, "Failure of a pressure regulator system by crevice corrosion: Attributed to improper material selection," *Journal of Failure Analysis and Prevention*, vol. 21, no. 1, pp. 22-27, 2021. https://doi.org/10.1007/s11668-020-01069-4

[16] K. Chu *et al.*, "Chloride stress corrosion cracking of a non-standard,'Borderline'Chromium-manganese stainless steel–problems of counterfeits and substandard materials," *Engineering Failure Analysis*, vol. 127, p. 105562, 2021. https://doi.org/10.1016/j.engfailanal.2021.105562

[17] H. Cheshideh, F. Nasirpouri, B. Mardangahi, and A. Jabbarpour, "Failure analysis and preventive recommendations against corrosion of steel tubes of gas risers in natural gas urban distribution lines," *Engineering Failure Analysis*, vol. 122, p. 105240, 2021. https://doi.org/10.1016/j.engfailanal.2021.105240

[18] N. Sreevidya, S. Abhijith, S. K. Albert, V. Vinod, and I. Banerjee, "Failure analysis of service exposed austenitic stainless steel pipelines," *Engineering Failure Analysis*, vol. 108, p. 104337, 2020. https://doi.org/10.1016/j.engfailanal.2019.104337

[19] Á. D. Bedoya-Zapata, C. M. Franco-Rendón, H. León-Henao, J. F. Santa, and J. E. G. Barrada, "Failure analysis of a welded stainless-steel piping system with premature pitting," *Engineering Failure Analysis*, vol. 119, p. 104986, 2021. https://doi.org/10.1016/j.engfailanal.2020.104986

[20] H. Tian *et al.*, "Effect of NH4+ on the pitting corrosion behavior of 316 stainless steel in the chloride environment," *Journal of Electroanalytical Chemistry*, vol. 894, p. 115368, 2021. https://doi.org/10.1016/j.jelechem.2021.115368

[21] S. Dong, X. Chen, E. C. La Plante, M. Gussev, K. Leonard, and G. Sant, "Elucidating the grain-orientation dependent corrosion rates of austenitic stainless steels," *Materials & Design*, vol. 191, p. 108583, 2020. https://doi.org/10.1016/j.matdes.2020.108583

[22] H. Ardy, T. Albatros, and A. Sumboja, "Failure analysis of duplex stainless steel for heat exchanger tubes with seawater cooling medium," *Metals*, vol. 13, no. 7, p. 1182, 2023. https://doi.org/10.3390/met13071182

[23] J. A. P. Nicacio, V. d. F. C. Lins, and A. Q. Bracarense, "Failure analysis in heat exchanger tubes from the top system of the regeneration tower of the hydrotreatment unit in an oil refinery: A case study," *Matéria Rio de Janeiro*, vol. 26, p. e13035, 2021. https://doi.org/10.1590/S1517-707620210003.13035

[24] M. Rezaei, Z. Mahidashti, S. Eftekhari, and E. Abdi, "A corrosion failure analysis of heat exchanger tubes operating in petrochemical refinery," *Engineering Failure Analysis*, vol. 119, p. 105011, 2021. https://doi.org/10.1016/j.engfailanal.2020.105011

[25] H. Wang, Y. Yang, Z. Yang, Z. Xu, Y. Chai, and Z. Zhang, "Corrosion failure analysis of duplex stainless steel in marine environment," *International Journal of Electrochemical Science*, vol. 17, no. 5, p. 22055, 2022. https://doi.org/10.20964/2022.05.52

[26] X. Yang, M. Liu, Z. Liu, C. Du, and X. Li, "Failure analysis of a 304 stainless steel heat exchanger in liquid sulfur recovery units," *Engineering Failure Analysis*, vol. 116, p. 104729, 2020. https://doi.org/10.1016/j.engfailanal.2020.104729

[27] X. Liu, H. Zhu, C. Yu, H. Jin, C. Wang, and G. Ou, "Analysis on the corrosion failure of U-tube heat exchanger in hydrogenation unit," *Engineering Failure Analysis*, vol. 125, p. 105448, 2021. https://doi.org/10.1016/j.engfailanal.2021.105448

[28] X. Wu, Y. Liu, Y. Sun, N. Dai, J. Li, and Y. Jiang, "A discussion on evaluation criteria for crevice corrosion of various stainless steels," *Journal of Materials Science & Technology*, vol. 64, pp. 29-37, 2021. https://doi.org/10.1016/j.jmst.2020.04.017